THE ASTROPHYSICAL JOURNAL, 455:335–341, 1995 December 10

HYDROGEN MOLECULES IN SN 1987A

MICHAEL CULHANE AND RICHARD MCCRAY
Joint Institute for Laboratory Astrophysics, University of Colorado and National Institute of Standards and Technology, Boulder, CO 80309-0440
Received 1994 July 5; accepted 1995 June 20

ABSTRACT

The observations of CO and SiO in the infrared spectrum of SN 1987A clearly indicate that molecules can form in the debris of a supernova explosion. Since H_2 is not easily observable we compute its abundance theoretically. For conditions typical of the inner ($v < 2500$ km s^{-1}) envelope of SN 1987A, the fraction of H that is in molecular form rises to $\sim 1\%$ by $t \sim 800$ days. For $t < 500$ days the formation is dominated by the gas-phase reactions $H + H^+ \rightarrow H_2^+ + h\nu$; $H_2^+ + H \rightarrow H_2 + H^+$. Thereafter, the formation is dominated by the reactions $H + e \rightarrow H^- + h\nu$; $H^- + H \rightarrow H_2 + e$. At early times the H^- may absorb $\sim 10\%$–30% of visible photons, contributing to the apparent paucity of Hα emission. For $t > 1000$ days the abundance of H_2 "freezes out" due to the slowing of all reactions. The opacity of the supernova envelope in the range $912 < \lambda \lesssim 1400$ Å (the upper limit depending on temperature) is dominated by resonance scattering in the Lyman and Werner bands of H_2. The resulting fluorescence emission bands of H_2 in the range $1150 < \lambda < 1650$ Å may be observable in the UV spectra of supernovae at late times.

Subject headings: line: formation — molecular processes — stars: individual (SN 1987A) — supernovae remnants — ultraviolet: ISM

1. INTRODUCTION

Spectroscopic observations of SN 1987A have enabled us to infer in unprecedented detail the physical conditions in its debris (McCray 1993). By $t \gtrsim 4$ months after the explosion, the optical/infrared photosphere had receded to the center of the envelope, and the spectrum was dominated by emission lines. Analysis of the spectra showed that the gas in the inner envelope was remarkably cool ($T \lesssim 3000$ K) and neutral (electron/neutral ratio $n_e/n_H \lesssim 0.02$), a fact evinced by the observation of emission bands of CO and SiO molecules as early as $t = 112$ days, well before any evidence for dust formation appeared. Evidently, the dense, cool, partially ionized gas in a supernova envelope is an environment favorable for molecule formation by gas-phase reactions (Dalgarno 1993). Thus, it is natural to ask whether H_2 molecules (or related species such as H_3^+) might also form there. Dalgarno (1993) has shown that the answer will be sensitive to the evolution of the temperature, density, and ionization in the envelope. Now that we have a better understanding of these conditions, we can revisit this question and model the formation of H_2 with more confidence.

Of course, we also want to know whether we can observe H_2 in the envelope of SN 1987A (or any other type II supernova). This may be difficult because the infrared decays of H_2 are so highly forbidden. We might also hope to detect H_2 in the UV through the strong Lyman and Werner emission bands, but that prospect is also clouded by the strong line blanketing (due primarily to iron group elements) that is seen in the UV spectra of supernovae. Nevertheless, there is evidence that this line blanketing diminishes at later times, opening windows in the UV spectrum where we might see H_2 emission bands.

Even if the UV radiation does not escape from the supernova envelope, there must be a substantial UV radiation field within the envelope of SN 1987A in order to account for the strengths of the hydrogen recombination lines (Xu et al. 1992) and the lines of Fe^+ (Li, McCray, & Sunyaev 1993). Today, our poor understanding of this UV radiation field is the greatest obstacle to a better understanding of the emission-line spectra of supernovae. As we shall show, H_2 molecules probably dominate the UV opacity of the inner envelope in the range $912 \lesssim \lambda \lesssim 1550$ Å. Thus, even if we fail to find direct evidence for H_2 in supernova envelopes, we must be able to model its abundance and UV opacity in order to understand the emission-line spectra of other species.

We address these questions here. In § 2 we define the model, including the conditions in the envelope of SN 1987A and the atomic processes that form and destroy H_2. Then, in § 3 we describe the resulting evolution of the abundances of H_2 and related species. In § 4 we describe a model for the production of UV radiation and its absorption and fluorescence by H_2. Finally, in § 5 we summarize our results and consider the implications for supernovae in general.

2. THE MODEL

2.1. *Physical Conditions*

Our present understanding of the structure and physical conditions in the envelope has been reviewed by McCray (1993). Here we summarize those facts relevant to the formation of H_2 molecules. We confine our discussion to the inner part (comoving with radial velocity $v \lesssim 2500$ km s^{-1}) of the supernova envelope that emits most of the optical/IR luminosity. Evidently, this region is an inhomogeneous mixture of "blobs" of nearly primordial composition separated from chemically distinct blobs of other element groups: He, O, Fe/CO/Ni, etc. We believe that dynamical instabilities during the first few hours or weeks after the explosion stirred up the stratified envelope of the progenitor star, resulting in an interior region with such a texture.

It is perhaps surprising that we can infer any quantitative information about the physical conditions in such a complex region. Yet fairly good fits to the evolution of the spectrum have been obtained with simple models in which each element group, with mass M_X, shares a fixed fraction, f_X, of the emitting volume and has uniform density $\rho_X(t) = 3M_X/(4\pi f_X v_1^3 t^3)$

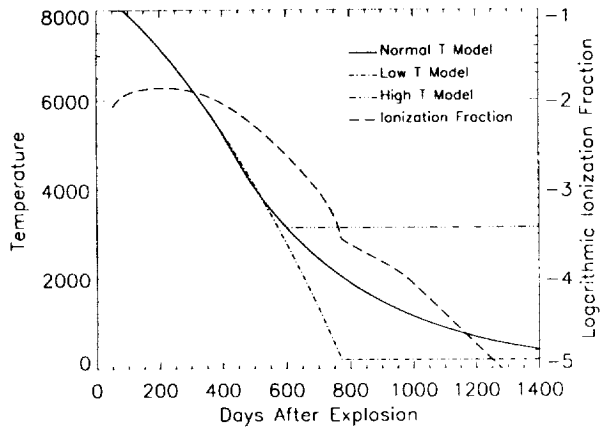

FIG. 1.—Models of temperature and ionization evolution

(where $v_1 = 2500$ km s^{-1}) and uniform temperature $T_X(t)$. For example, Xu et al. (1992) showed that this inner region must contain $M_H \sim 3$–$7\ M_\odot$ of hydrogen, filling $f_H \sim 0.5$ of the emitting volume, in order to produce hydrogen recombination lines with the observed strengths and widths. (We choose $f_H = 0.5$ because Li et al. 1993 showed that the Fe/Co/Ni blobs must expand to fill $f_{Fe} \sim 0.5$ of the emitting volume.) Xu et al. also inferred the evolution of the hydrogen ionized fraction, $x_H = n(H^+)/n(H)$, from the emission measure. Figure 1 shows this function, which we use for our model calculations.

The hydrogen recombination rate coefficients are fairly insensitive to temperature, so it is difficult to infer the evolution of the hydrogen temperature, $T_H(t)$, from the strengths of the recombination lines. However, Li & McCray (1993) showed that the strong [Ca II] $\lambda\lambda$7300 and Ca II $\lambda\lambda$8600 lines must come from material with primordial abundance ratio of Ca/H, amost certainly the hydrogen-rich gas. Since the strengths and ratios of the Ca II lines are sensitive to temperature, one can infer $T_H(t)$ from the results of Li & McCray (1993). This function is plotted as the solid curve in Figure 1. The Ca II lines are not bright enough to provide a reliable estimate of $T_H(t)$ for $t \gtrsim 600$ days, however. Therefore, we consider three alternatives for the late-time development of $T_H(t)$, shown on Figure 1. The first (*the extension of the solid curve*) is a simple exponential decay with mean life 400 days. The second alternative (*the dashed curve*) simply assumes that the temperature remains constant for $t \gtrsim 600$ days; and the third (*the dot-dashed curve*) assumes a linear decrease of temperature for $t \gtrsim 600$ days. We think that the latter two alternatives probably bracket the actual function.

2.2. *Molecule Formation and Destruction*

Hydrogen molecules are produced in supernova envelopes by gas-phase reactions involving H^- and H^+ and possibly also by formation on dust grains. They are destroyed by thermal collisions, fast electrons resulting from gamma-ray energy deposition, and ultraviolet radiation. The reactions and rate coefficients responsible for producing and destroying H_2 are listed in Table 1.

Since we know that dust graints formed in the envelope of SN 1987A after $t \sim 400$ days (McCray 1993), we should examine whether dust grain catalysis (reaction 1 of Table 1) might compete with gas-phase reactions in producing H_2. The production rate per unit volume of H_2 molecules by dust catalysis is given by kN_H^2, where the rate coefficient can be written

$$k = [N_{gr}\sigma_{gr}/N_H]\langle Sv\rangle f\ , \qquad (1)$$

where N_{gr} is the grain density, σ_{gr} is the average grain geometrical cross section, $\langle Sv\rangle$ is the thermal average of the sticking coefficient, and f is the fraction of the H atoms that form a molecule (presumably, at an impurity site) before evaporating from the grain. According to Hollenbach & McKee (1979), we have

$$\langle Sv\rangle \approx v_{th}/[1 + 0.04(T + T_{gr})^{0.5} + 0.002T + 8 \times 10^{-6}T^2]\ \text{cm}^3\ \text{s}^{-1} \qquad (2)$$

TABLE 1

REACTIONS FOR H_2 FORMATION AND DESTRUCTION

Reaction	Rate Coefficient (cm^3 s^{-1})	Reference
(1) $2H + \text{grain} \rightarrow H_2 + \text{grain}$	...	See § 2
(2) $H + H^+ \rightarrow H_2^+ + h\nu$	4.1×10^{-17}	1
(3) $H_2^+ + H \rightarrow H_2 + H^+$	1.0×10^{-10}	2
(4) $H_2^+ + H_2 \rightarrow H_3^+ + H$	2.1×10^{-9}	2
(5) $H_2^+ + e \rightarrow 2H$	$2.25 \times 10^{-6}T^{-0.4}$	3
(6) $H_3^+ + e \rightarrow 3H$	$1.7 \times 10^{-7}T^{-0.5}$	2
(7) $H_3^+ + e \rightarrow H + H_2$	$1.7 \times 10^{-7}T^{-0.5}$	2
(8) $H + e \rightarrow H^- + h\nu$	$1.0 \times 10^{-18}T \exp(-T/7000)$	4
(9) $H^- + H \rightarrow H_2 + e$	1.3×10^{-9}	2
(10) $H^- + H^+ \rightarrow 2H$	$1.1 \times 10^{-6}T^{-0.4}$	4
(11) $H^* + H \rightarrow H_2 + h\nu$	4×10^{-14}	5
(12) $H^* + H \rightarrow H_2^+ + e$	1.2×10^{-11}	6
(13) $H^* + H_2 \rightarrow H_3^+ + e$	$1.6 \times 10^{-11}T^{0.5}$	7
(14) $H_2 + H \rightarrow 3H$	$7.0 \times 10^{-18}F(n, T)$[a]	8
(15) $H_2 + \text{fast } e \rightarrow H_2^+ + 2e$	...	See § 3
(16) $H_2 + \text{fast } e \rightarrow H + H^+ + 2e$	...	See § 3
(17) $H_2 + h\nu \rightarrow 2H$	...	See § 4

[a] $F(n, T)$ is a sensitive function of density and temperature [$F(n, T) \sim 1$ at $T = 3000$ K] given in Fig. 1 of Dalgrano & Roberge (1979).

Chemistry rate sources: (1) Ramaker & Peek 1976; (2) Tielens & Hollenbach 1985; (3) de Jong 1972; (4) Shapiro & Kang 1987; (5) Latter & Black 1991; (6) Urbain et al. 1991; (7) Chupka et al. 1967; (8) Dalgarno & Roberge 1979.

and

$$f = [1 + N_t/N_i \exp(-D/kT_{gr})]^{-1}, \quad (3)$$

where $v_{th} = (3kT/m_H)^{1/2}$, $N_t/N_i \approx 10^4$ is the number of collisions before an atom directly strikes an impurity, and the binding energy $D/k \approx 600$ K.

Knowledge of the evolution of hydrogen atomic density, ionized fraction, and temperature is sufficient to determine the production rate of H_2 by the gas-phase reactions (2–13) of Table 1, except that the abundance of H^- is suppressed by photodetachment (the inverse of reaction 8). This photodetachment is dominated by the radiation field in the band $4000 < \lambda < 12000$ Å, which we infer from the observed spectrum in this range, assumng that it emanates from a sphere bounded by the $v = 2500$ km s^{-1} comoving surface. The rate of production, R_d, of photons capable of detaching electrons from H^- is related to the emergent flux of such photons, F_d (cm^{-2} s^{-1} Å^{-1}) by

$$R_d = 4\pi D^2 F_d / P_\lambda, \quad (4)$$

where D is the distance to the supernova,

$$P_\lambda = \frac{3}{4\tau_\lambda}\left[1 - \frac{1}{2\tau_\lambda^2} + \left(\frac{1}{\tau_\lambda} + \frac{1}{2\tau_\lambda^2}\right)e^{-2\tau_\lambda}\right] \quad (5)$$

is the mean escape probability (Osterbrock 1989), and τ_λ is the optical depth to the center of the sphere due to H^-. Therefore, the number of dissociations per second of H^- is $(1 - P_\lambda)(4\pi D^2 F_d/P_\lambda)$.

Hydrogen molecules can be destroyed by collisions with thermal hydrogen atoms; the rate coefficient for reaction 14 (including radiative stabilization) is given by Dalgarno & Roberge (1979).

In the supernova envelope, gamma rays and positrons from the decays of ^{56}Co and ^{57}Co produce suprathermal electrons that can ionize hydrogen atoms and dissociate H_2 molecules. According to Xu et al. (1992), the ionization of hydrogen atoms is dominated by fast electron stopping for $t \gtrsim 375$ days, and so we may infer the corresponding ionization rate, ζ_H, from the strengths of the observed recombination lines. Then, the dissociation rate, ζ_{H2}, per hydrogen molecule by fast electrons can be written $\zeta_{H2} = (\langle\sigma_{H2} v\rangle/\langle\sigma_H v\rangle)\zeta_H$, where the ratio of the effective cross sections $(\langle\sigma_{H2} v\rangle/\langle\sigma_H v\rangle) = 2.0$ (Tielens & Hollenbach 1985).

Finally, we must consider the dissociation of H_2 resulting from resonance absorption of ultraviolet photons in the Lyman and Werner bands. A fraction ~ 0.10 of these absorptions will result in decay to the vibrational continuum. In its ground vibrational state, H_2 can only absorb UV photons in the range $912 < \lambda < 1108$ Å, but at the high temperature of the supernova envelope the presence of vibrationally excited H_2 molecules can extend the upper bound to ~ 1600 Å. In order to calculate the rate of photodissociation by this process, we must consider in detail the origin and transfer of the UV radiation field. We shall address this problem in § 4.

3. MOLECULE FORMATION AND ABUNDANCES

Figure 2 shows the evolution of the H_2 mass fraction, $f(H_2) = 2n(H_2)/n(H)$ for five models. The solid curve represents our nominal model A, characterized by $M_H = 5\ M_\odot$ of hydrogen in the emitting region and a temperature profile given by the solid curve in Figure 1. To assess the sensitivity of the results to atomic density we consider also two models having

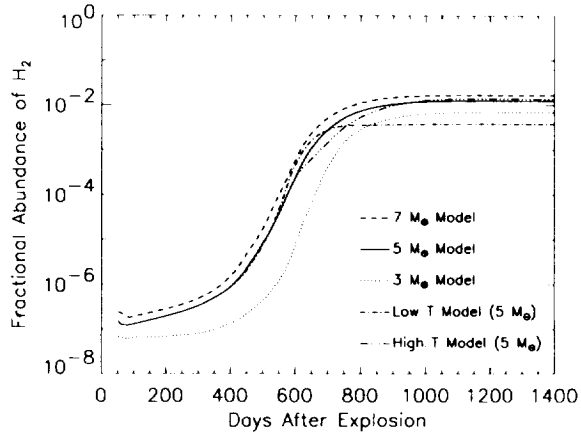

FIG. 2.—Fractional mass of hydrogen molecules as a function of time for various models.

the same temperature evolution but with $M_H = 3\ M_\odot$ (model B) and $M_H = 7\ M_\odot$ (model C). To assess the sensitivity to the temperature evolution for $t > 600$ days we consider two more models, both with $M_H = 5\ M_\odot$ but temperature after $t = 600$ days decreasing more rapidly (model D) or remaining constant (model E), as illustrated in Figure 1.

As Figure 2 shows, in every case $f(H_2)$ rises rapidly at $t \sim 600$ days and by $t \sim 900$ days reaches an asymptotic value $f(H_2) \approx 10^{-2}$. With increasing M_H, $f(H_2)$ rises somewhat earlier, but the asymptotic value of $f(H_2)$ depends only weakly on M_H. The H_2 production is sensitive to the behavior of temperature at late times. If the temperature drops rapidly, less H_2 is formed, as illustrated by curve E.

We can understand these results by looking more closely at the processes responsible for forming and destroying H_2. To do this, we write the equation for evolution of the H_2 abundance in the form

$$\frac{dn(H_2)}{dt} = F - Dn(H_2), \quad (6)$$

where F represents all the processes responsible for forming H_2 (resulting from the reactions listed in Table 1), and the net destruction rate, $Dn(H_2)$, represents all the processes responsible for destroying H_2 (reactions 14–17 of Table 1).

Then, we can define expressions representing the age of the supernova divided by the characteristic timescales for formation and destruction at follows:

$$R_F = t\frac{F}{n(H_2)} \quad (7)$$

and

$$R_D = tD. \quad (8)$$

These quantities, as well as the net formation rate, $R_F - R_D$, are plotted in Figure 3 for model A. For $t \lesssim 600$ days, both R_F and R_D are $\gg 1$, i.e., the population of H_2 is formed and destroyed many times during the age of the supernova. Therefore, the abundance of H_2 reaches a stationary equilibrium, $f(H_2) = F/[n(H)D]$. But for $t \gtrsim 600$ days the destruction rate decreases more rapidly than the formation rate and the H_2 abundance builds up rapidly. This process continues until $t \sim 1000$ days; thereafter the formation timescale is longer than the age of the supernova ($R_F < 1$ in Fig. 3) and the abundance "freezes out."

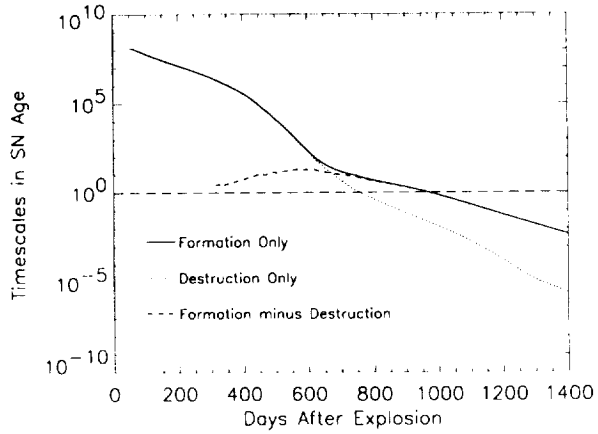

FIG. 3.—Formation rate, R_F (*solid curve*), destruction rate, R_D (*dotted curve*), and net formation rate, $R_F - R_D$ (*dashed curve*) of hydrogen molecules.

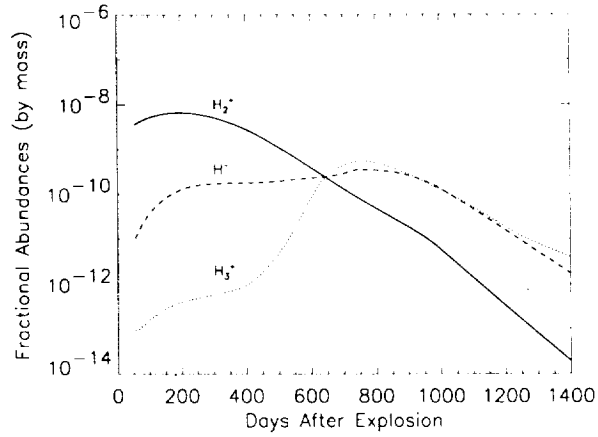

FIG. 5.—Abundances of H^-, H_2^+, H_3^+, and H_2 as fractions of the total hydrogen mass.

Figure 4 shows, for model A, the contributions of various processes for formation and destruction of H_2 as fractions of the respective total rates. We see that the reactions (2, 3, and 12) dominate the formation for $t \lesssim 500$ days, but that the H^- reactions (8, 9) dominate for $t \gtrsim 500$ days, when most of the H_2 is formed. Formation on dust grains (reaction 1, the dominant mechanism in diffuse interstellar clouds) or by the H* process (reaction 11) never makes a significant contribution. Figure 4 also shows that the UV photodissociation dominates the destruction of H_2 except for $t \gtrsim 1200$ days, by which time the destruction timescale is much greater than the age of the supernova. In fact, the asymptotic abundance of H_2 is insensitive to the UV field, because the UV photodissociation rate is negligible compared to the formation rate when the H_2 abundance freezes out.

Figure 5 shows, for model A, the mass fractions of the important trace ions, H^-, H_2^+, and H_3^+ as functions of time. The abundance of H^- is controlled largely by a balance between the radiative attachment reaction (8) and, for $t \lesssim 600$ days by its inverse, where the photodetachment is dominated by the strong Hα, O I $\lambda\lambda$6300, [Ca II] $\lambda\lambda$7300, and Ca II $\lambda\lambda$8600 lines seen in the observed radiation field. For $t \gtrsim 600$ days, the H^- is destroyed primarily by forming H_2 (reaction 9). We see that $f(H^-) = n(H^-)/n(H) \approx 10^{-10}$ until $t \approx 1000$ days, after which it decreases. The H_3^+ is formed by reaction (4) and destroyed by reactions (6) and (7); therefore its abundance rises rapidly for $t \gtrsim 600$ days along with the abundance of H_2. The reaction rates (6) and (7) are relatively uncertain and the value chosen for these rates can dramatically change the final abundance of H_3^+. We will return to this point in § 5.2.

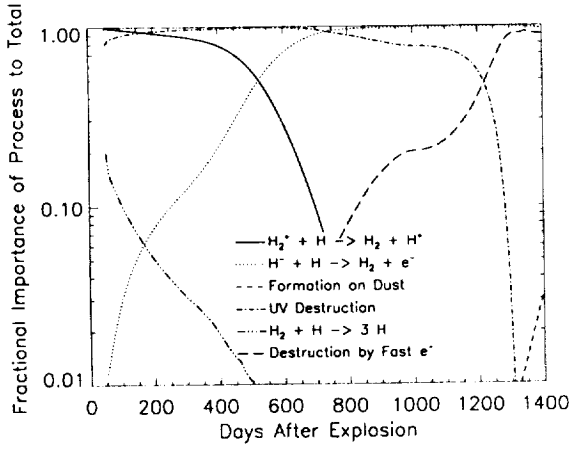

FIG. 4.—Processes that contribute significantly to formation or destruction of hydrogen molecules. Curves indicate rate of individual process as fractions of the total formation or destruction rate.

4. ULTRAVIOLET FLUORESCENCE

4.1. *The Model*

A few weeks after the explosion, the supernova envelope can be regarded as a freely expanding sphere of gas (McCray 1993). Accordingly, the relative velocity, Δv, of any two atoms or molecules in the envelope is related to their separation, Δr, by a Hubble law, $\Delta v = H_0 \Delta r$, where the Hubble constant is related to the age of the supernova by $H_0 = t^{-1}$. Likewise, the wavelength of radiation emitted by an atom at one point and absorbed by an atom at another point is redshifted according to the Hubble law.

As a result of illumination by gamma rays, metastable $2\ ^1S$ state of hydrogen and helium in the supernova envelope are populated by nonthermal electron impact excitation and recombination. The metastable hydrogen population is elevated because the Lyα transition is suppressed due to the very high optical depth of the line (Xu et al. 1992). Consequently, the metastable helium and the metastable hydrogen both decay by two-photon emission, and these decays are the main sources of UV continuum photons within the supernova envelope.

Observations of the spectra of supernovae, and SN 1987A in particular, show that, unlike the optical and infrared radiation, most of this UV radiation does not escape the supernova envelope. For $\lambda < 912$ Å, the UV radiation is strongly absorbed by photoionization of H I. For $912 < \lambda \lesssim 3000$ Å it is absorbed by resonance transitions of trace elements such as Fe I and Fe II (Mazzali & Lucy 1991; Xu & McCray 1991). As we shall show, the Lyman and Werner transitions of H_2 probably dominate the UV opacity in the range $912 \lesssim \lambda \lesssim 1400$ Å, where the upper limit is sensitive to temperature. As we describe below, these transitions convert the H I and He I two-photon continuum photons emitted in this range into photons of longer wavelength by fluorescence and also dissociate the molecules.

4.2. *Method of Calculation*

First, we must calculate the source function for two-photon continuum photons in the emitting region. For hydrogen, we

use the results of Xu et al. (1992), who calculate the population of metastable hydrogen atoms, H*, in the inner envelope. To calculate the two-photon emissivity we assume that $\frac{1}{4}$ of the hydrogen atoms in the $n = 2$ state are in the $2\,^2S$ state. The H* atoms decay with a spectrum (Nussbaumer & Schmutz 1984) that peaks at 1420 Å. Li & McCray (1995a) have calculated models for the production of two-photon continuum from metastable helium in the envelope of SN 1987A. Its spectrum (Drake, Victor, & Dalgarno 1969) peaks at ~800 Å. Note that the He I two-photon continuum is produced only in the part of the envelope composed of nearly pure helium. The primordial helium that is mixed with the hydrogen will not produce a two-photon continuum because the He* is depopulated rapidly by Penning ionization of H I. Because the He I two-photon continuum comes from regions geometrically separated from the H I regions, there is some uncertainty as to whether the He I two-photon continuum will illuminate the H_2—it may be absorbed by metals before it propagates into the hydrogen. We do not attempt to model this effect, however.

Given the two-photon continuum source function, we must model its transfer through the envelope. We are interested in photons in the spectral range $912 < \lambda \lesssim 1800$ Å where resonance transitions of H_2 molecules dominate the opacity and fluorescence emissivity. To calculate the transfer of such photons, we use a Monte Carlo code. This simulation proceeds as follows. First, we introduce a continuum photon in this band chosen at random with weight proportional to the two-photon continuum spectrum of the metastable hydrogen or helium. Its position within the $v = 2500$ km s^{-1} sphere and initial propagation direction are also random.

As the photon propagates, it redshifts with respect to the comoving matter according to the Hubble law. Thus, we can define a sequence of concentric spherical "resonance shells" around the point of origin of the photon with radial velocities given by the respective redshifts from the source photon wavelength to the resonance lines, $\lambda_{i,j}$, in the Lyman or Werner bands to the red of the source photon wavelength, λ_0.

Next, we must decide which, if any, resonance shell will capture the source photon. The transmission probability for a photon to penetrate any given resonance shell is given by

$$T_{i,j}(\tau) = \exp(-\tau_{i,j}), \tag{9}$$

where the optical depth, $\tau_{i,j}$, of the line is given by the Sobolev approximation (Castor 1970; McCray 1993),

$$\tau_s = \frac{\pi e^2}{m_e c} f_{ij} \lambda_0 t n_i \left[1 - \frac{g_i n_j}{g_j n_i}\right] = \frac{\lambda_0^3 t g_u A_{ji} n_i}{8\pi g_i} \left[1 - \frac{g_i n_j}{g_j n_i}\right], \tag{10}$$

where n_j, g_j, n_i, g_i are number densities and statistical weights of atoms in the upper and lower states, respectively, on the resonant surface. According to equation (10), $\tau_{i,j}$ depends only on n_i and the oscillator strength of the transition i, j (we used the molecular data found in Abgrall & Roueff 1989 and Abgrall et al. 1992). (One can assume safely that these levels are populated with a Boltzmann distribution.) We choose a value $\tau_1 = -\ln(T_1)$, where T_1, the transmission probability, is a random number, $0 < T_1 < 1$. The wavelength, λ_1, of the first resonance scattering is then given by the condition

$$\sum_{\lambda_{i,j}=\lambda_0}^{\lambda_1} \tau(\lambda_{i,j}) > \tau_1, \tag{11}$$

i.e., the first resonance scattering occurs at the wavelength $\lambda_{i,j}$ for which the accumulated Sobolev optical depth of all intervening resonance shells just exceeds τ_1.

If, for the chosen direction of propagation, the resonance shell where the scattering occurs lies beyond the $v = 2500$ km s^{-1} surface, the photon is deemed to have escaped and is stored in the emergent spectrum file. Otherwise, a new photon is generated at the location of the resonance scattering, with direction and wavelength assigned at random according to the branching ratios of the radiative decays. Typically, ~10% of these decays result in dissociations to the vibrational continuum. To account for these transitions, we assign the resulting continuum photon an energy less than that of the lowest energy bound-bound transition by one lower vibrational quantum. This approximation is sufficient for our purposes because the continua are peaked near threshold. Then, we define a new set of resonance shells concentric on the location where the new photon is generated and repeat the process until no further scatterings are possible.

4.3. *Results*

Figure 6 shows the emergent spectrum that results from UV fluorescence by H_2 molecules for model A at $t = 500$ days. The fuzzy curve represents the input UV continuum, as generated by the Monte Carlo code. Both the H I and He I two-photon continua are evident. The solid curve is the emergent spectrum resulting from blocking by the Lyman and Werner bands of H_2. Because many transitions from the $v = 0$, 1, 2 levels of the ground electronic ($^1\Sigma_g^+$) state of H_2 have high Sobolev optical depths, H_2 resonance scattering blocks almost all continuum photons with $\lambda \lesssim 1470$ Å. The blocked UV photons are ultimately converted (sometimes after several resonance scatterings) to H_2 emission bands and continua in the range $1470 \lesssim \lambda \lesssim 1720$ Å.

Figure 7 shows the input and emergent spectra for model A at $t = 1200$ days. The H I two-photon continuum has vanished because the Lyα optical depth has decreased enough to favor that channel for decay of H*, and the input continuum spectrum is dominated by the He* two-photon continuum. The envelope has now become mostly transparent for $\lambda \gtrsim 1200$ Å, primarily because the temperature has dropped and so have the populations of the $v > 1$ levels of the H_2, and secondarily because the envelope has become thinner [for fixed fractional abundances, $\tau(\lambda_{i,j}) \propto t^{-2}$].

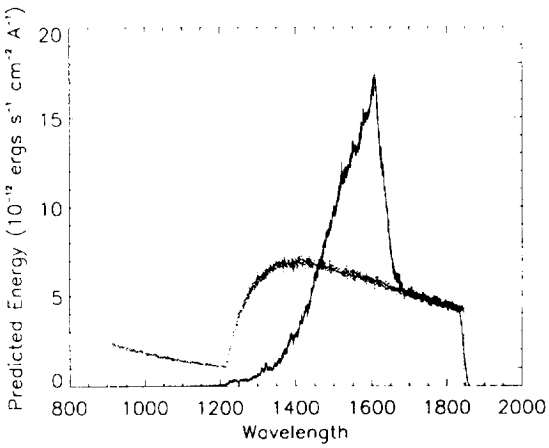

FIG. 6.—Fluorescence spectrum of H_2 at 500 days. Dotted (*lighter*) line gives spectrum produced by He and H two-photon emission in the region of interest assuming no absorption. Solid line shows the same spectrum emitted from a uniform sphere of He and H and shining through a coincident uniform sphere of H_2. Spectrum is computed using the values of emission, temperature, and H_2 density at 500 days of the 5 $M_\odot$ model.

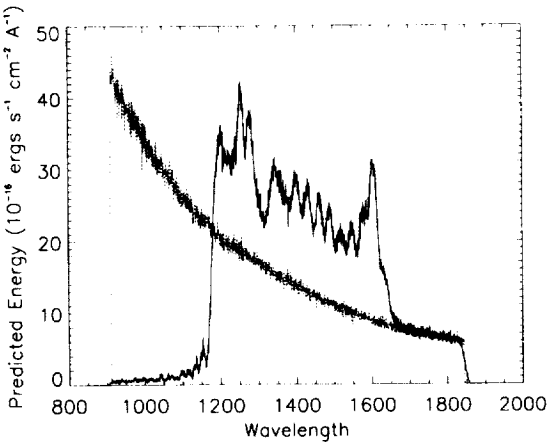

FIG. 7.—Fluorescence spectrum of H_2 at 1200 days. Same as Fig. 6 except conditions are those of the 5 $M_\odot$ model at 1200 days.

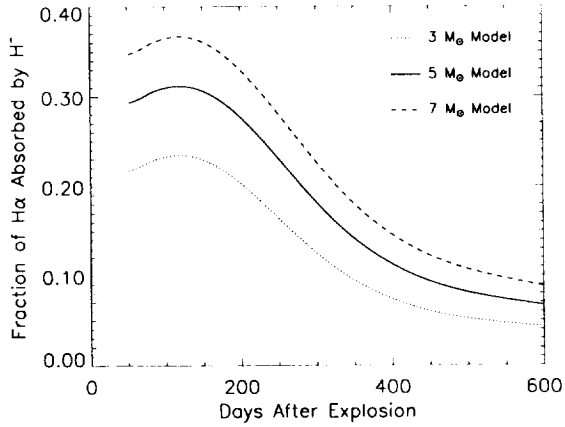

FIG. 8.—Significance of H^- opacity to the optical spectrum at early times. Curves give the fraction of Hα absorbed by H^-.

The fluorescence spectrum is created primarily through transitions involving the lower vibrational states of the Lyman and Werner bands. For example, the peak at 1600 Å is created primarily through transitions from upper levels with $v' = 3$–6 to lower levels with $v = 10$–13. The other peaks all have strong transitions from $v' = 0$ to v ranging from 2 (1250 Å peak) to 7 (1550 Å peak). Some H_2 emission features do not appear in the spectrum because the photons are absorbed by transitions at slightly longer wavelengths. Note that a transition with $\tau \gg 1$ does not necessarily absorb more photons than a transition with $\tau \sim 1$. If there are many optically thick transitions within a few Å of each other, then the absorption of the continuum (and fluorescence photons) emitted in that region will be shared by all of those transitions. On the other hand, an optically thin line that is not close to any other optically thick absorption lines will absorb $[1 - \exp(-\tau)]$ of all photons emitted in that region.

At 1200 days there are 0.35 fluorescence photons, 0.088 dissociations, and 0.51 absorptions for each He continuum photon in the range 912–1850 Å. At 500 days the interaction with the radiation field is much stronger, with 2.2 absorptions, 0.2 dissociations, and 0.69 fluorescence photons in the spectrum for each He continuum photon emitted (in the same wavelength range). Note that because a vibrational continuum photon is emitted when the molecule is dissociated, one He continuum photon can dissociate more than one molecule. Moreover, an individual photon can be absorbed many times on its way through the envelope. However, when a photon is reemitted by the same transition by which it is absorbed, we have not counted this as a separate absorption (this is one reason, perhaps the main reason, that the dissociation rate per absorption changes from 0.11 at 500 days to 0.17 at 1200 days).

5. DISCUSSION

5.1. H^- *Opacity and the Deficit of* Hα

Xu et al. (1992) find the Hα emission to be about half that which would be implied by the strength of the infrared recombination lines. As one possible explanation, they suggest that the Hα may be absorbed by H^-. According to our model, H^- is a significant absorber of Hα. For $t \lesssim 300$ days after explosion, the predicted H^- can absorb up to 30% of the Hα emission (Fig. 8). This absorption is not enough to explain the discrepancy between the observed and expected Hα emission, however.

Alternatively, Xu et al. (1992) suggest that the deficit of Hα emission may result from the absorption of Lyβ by a nearby resonant absorption line. Could the hydrogen molecules produce such a line? In fact, there are ~100 such lines within 1 Å of Lyβ. These lines have a net Sobolev optical depth of about 25 at 200 days, which increases to ~190 at 500 days. However, at $t = 1$ yr, the Lyβ optical depth, $\tau(\text{Ly}\beta) \sim 10^{10}$ and $\tau(\text{H}\alpha) \sim 10^4$ (Xu et al. 1992). As a result, each Lyβ photon is absorbed by hydrogen atoms rather than by hydrogen molecules (after 10^4 Hα scatterings only $\sim 10^{-5}$ of the Lyβ photons will be lost to hydrogen molecules). The rest will be trapped until they diffuse to the wings of Hα and escape. So, even after correcting for the absorption due to H^- and H_2, the Hα deficit remains an unsolved puzzle.

5.2. H_2 *and* H_3^+ *Infrared Emission*

Meikle et al. (1993) see a very weak feature at 2.12 μm which they tentatively identify as the $v(1 \rightarrow 0)S(1)$ transition of H_2. Although it is not clear that this identification is correct, the observations should provide an upper limit for the 2.12 μm flux produced by our models. Figure 9 shows the observed upper limits and the fluxes produced by our models. The models indicate that if the hydrogen ejecta mass $M_H \gtrsim 5\ M_\odot$, our assumed temperature is too high to be consistent with the

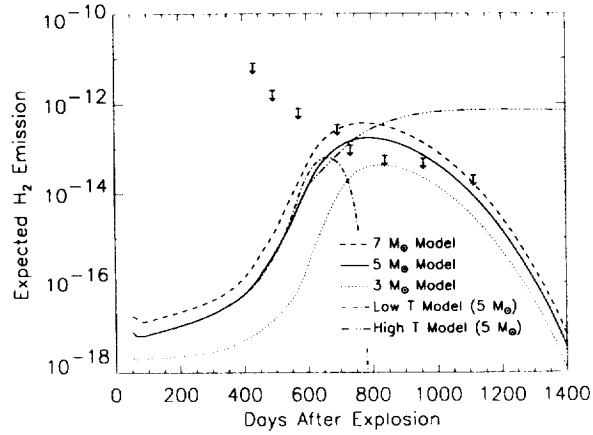

FIG. 9.—H_2 $v(1 \rightarrow 0)S(1)$ emission from SN 1987A. Crosses give upper limit of 2.12 μm emission from SN 1987A. Curves give emission predicted by various models.

upper limit. We can also see that H_2 emission could in fact be producing much of the observed flux at 2.12 μm for $t \gtrsim 600$ days. Unfortunately, none of the other infrared transitions is bright enough to be seen over the continuum, so we cannot confirm whether the observed feature actually comes from H_2.

Miller et al. (1992) have suggested that weak emission features observed at about 3.41 and 3.53 μm in the spectrum of SN 1987A at $t = 192$ days are produced by H_3^+. They find that $\sim 10^{-8}\ M_\odot$ of H_3^+ is required to produce the observed line strengths. Yan, Dalgarno, & Lepp (1994) report that their model calculations yield a fractional abundance (at $t = 192$ days) $n(H_3^+) \sim 10^{-8} n(H)$, dramatically higher than our result $n(H_3^+) \sim 10^{-13} n(H)$. Most of the difference can be traced to the fact that our calculated H_2 abundance at that time is orders of magnitude lower than that calculated by Yan et al. This is true because (1) Yan et al. did not include the rapid photodissociation of H_2 by UV continuum; and (2) our assumed gas temperature at that time (Fig. 1) is much greater than the value $T = 1000$ K assumed by Yan et al., and so the thermal dissociation rate of H_2 (Table 1, reaction 14) is much greater in our model. In our calculations, the H_3 abundance reaches a maximum value $n(H_3^+) \sim 10^{-10} n(H)$ at $t \approx 700$ days, far too low to cause a detectable infrared emission feature.

We conclude that if the 3.41 and 3.53 μm features in the spectrum of SN 1987A are produced by H_3^+, two assumptions of our model must be invalid: (1) the UV continuum from two-photon decay of H I and He I illuminates the H_2; and (2) the temperature of the hydrogen in the envelope of SN 1987A can be inferred from the brightness of the infrared lines of Ca II (Li & McCray 1993). If assumption (1) is invalid, there must be some other very effective source of UV opacity that protects the H_2. If assumption (2) is invalid, we have no model to account for the observed brightness of the Ca II lines.

5.3. H_2 *Ultraviolet Fluorescence*

In § 4 we showed that resonance fluorescence by H_2 will substantially alter the emergent ultraviolet spectrum. Emission features characteristic of H_2 fluorescence (Figs. 6, 7) have not been observed in the UV spectrum of SN 1987A, however.

We suspect that the absence of such features can be attributed to the blocking of this radiation by many lines of Fe and other metals in the supernova envelope (Mazzali & Lucy 1991; Xu & McCray 1991). It is possible, however, that at some future time the UV line blocking may diminish enough to provide a spectral window through which we could see the H_2 fluorescence.

As we mentioned in § 1, we need to model the formation and transfer of the UV radiation field in supernova envelopes in order to understand fully the optical and infrared emission-line spectrum. Here, we have shown that H_2 line blocking and fluorescence play an important role in the transfer of UV radiation, but our task is incomplete. Resonance lines of ions of Fe and other metals will also trap UV radiation and convert it to longer wavelengths (Li & McCray 1995b). Since the H_2 molecules are far more abundant than the metals, they should dominate the opacity at those wavelengths where the H_2 bands are opaque (see Figs. 6 and 7). But the metals might prevent the escape of the H_2 fluorescence bands. To see what fraction of the H_2 fluorescence escapes, we need a detailed calculation of ultraviolet trapping and fluorescence, including both metals and molecules. That will be our next step.

This work was supported by the NASA Astrophysical Theory Program through grant NAGW-766 and by NASA grant NAGW-2900. We thank E. Roueff for providing us with data on the UV radiative transitions of H_2.

REFERENCES

Abgrall, H., Le Bourlot, J., Pineau des Forets, G., Roueff, E., Flower, D. R., & Heck, L. 1992, A&A, 253, 525
Abgrall, H., & Roueff, E. 1989, A&AS, 79, 313
Castor, J. 1970, MNRAS, 149, 111
Chupka, W. A., Russel, M. E., & Refaev, K. 1967, J. Chem. Phys., 48, 1518
Dalgarno, A. 1993, in Dissociative Recombination: Theory Experiment and Applications eds. B. R. Rowe, J. B. A. Mitchell, & A. Canosa (New York: Plenum), 243
Dalgarno, A., & Roberge, W. B. 1979, ApJ, 332, L25
de Jong, T. 1972, A&A, 20, 263
Drake, G. W. F., Victor, G. A., & Dalgarno, A. 1969, Phys. Rev., 180, 25
Hollenbach, D., & McKee, C. F. 1979, ApJS, 41, 555
Latter, W. B., & Black, J. H. 1991, ApJ, 372, 161
Li, H., & McCray, R. 1993, ApJ, 405, 730
———. 1995a, ApJ, 441, 821
———. 1995b, ApJ, 455
Li, H., McCray, R., & Sunyaev, R. 1993, ApJ, 419, 824
Mazzali, P. A., & Lucy, L. B. 1991 in Evolution in Astrophysics, *IUE* Toulouse Symposium, ed. E. Role (ESA SP-310), 483
McCray, R. 1993, ARA&A, 31, 175
Meikle, W. P. S., Spyromilio, J., Allen, D. A., Varani, G.-F., & Cumming, R. J. 1993, MNRAS, 261, 535
Miller, S., Tennyson, J., Lepp, S., & Dalgarno, A. 1992, Nature, 355, 420
Nussbaumer, H., & Schmutz, W. 1984, A&A, 138, 495
Osterbrock, D. E. 1989, Astrophysics of Gaseous Nebulae and Active Galactic Nuclei (Mill Valley, Ca: University Science Books), 386
Ramaker, D., & Peek, J. 1976, Phys. Rev. A, 13, 58
Shapiro, P., & Kang, H. 1987, ApJ, 318, 32
Tielens, A. G. G. M., & Hollenbach, D. 1985, ApJ, 291, 722
Urbain, X., Cornet, A., & Brouillard, F. 1991, Phys. Rev. Lett., 66, 1685
Xu, Y., & McCray, R. 1991, in Supernovae, ed. S. E. Woosley (New York: Springer), 444
Xu, Y., McCray, R., Oliva, E., & Randich, S. 1992, ApJ, 386, 181
Yan, M., Dalgarno, A., & Lepp, S. 1994, BAAS, 26, 953